APPLICATION OF QUANTITATIVE MICROFRACTOGRAPHY IN DAMAGE-TOLERANCE AND FATIGUE EVALUATION OF WING SPAR

Jiří Kunz*, Jan Siegl*, Ivan Nedbal*, Petr Augustin, Antonín Píštěk****
***Czech Technical University in Prague, **Brno University of Technology, Czech Republic**

Keywords: *damage-tolerance, fatigue, full-scale test, wing spar, quantitative fractography*

Abstract

Experimental study was focused on the fatigue crack propagation in a model of the Ayres Loadmaster LM 200 wing spar. During a high-cycle full-scale fatigue test, the monotonic four point cyclic bending was applied. Fatigue crack growth in the spar web was visually monitored, but the measurement was not possible as long as the flange plate coved the web. The limited macroscopic data set was completed by the fractographic reconstitution of fatigue crack history based on the striation spacing measurement. During the fractographic data processing, various hypotheses were applied. Synthesis of macroscopic data with the fractographic ones gives detailed information on the real course of the fatigue process in the critical area (e.g., time sequence of individual fatigue cracks, their interaction etc.). Similar information on locations and modes of damage due to fatigue are substantial for damage-tolerance evaluation of structure components.

1 Introduction

According to [1], a special consideration for wide spread fatigue damage must be included in the damage-tolerance evaluation. Probable locations and modes of fatigue damage should be demonstrated with sufficient full-scale test evidence. The efficiency of these exacting and expensive experiments can be considerably increased by application of quantitative fractography. Whereas possibilities of visual monitoring methods are limited (especially in the case of hidden and inaccessible cracks), fractography can give precious supplementary data. Information encoded in fracture micro-morphology is objective and often unobtainable in other ways. By the methods of fractographic reconstitution, it is possible to obtain detailed information on the fatigue process in the tested structure parts - e.g., crack initiation length; crack growth rates in various locations of the fatigued area; time-dependent, two-dimensional description of fatigue crack growth; time sequence of individual failures and their interaction; consequences of applied repairs etc. [2]. In addition to the assets mentioned, the quantitative fractography is indispensable for the study of fundamental principles of fatigue mechanisms [3], for the evaluation of prediction models of fatigue crack growth under variable amplitude loading [4], etc. These possibilities are conditioned by the existence and measurability of fractographic features some quantitative characteristic of which is correlated with the crack growth rate. Suitable features are especially striations [5], [6] and beach marks associated with the most severe applied cycles, e.g., marker bands corresponding to specific marking cycles or blocks in the loading spectrum [7]-[9]. If it is possible to distinguish individual striations and to measure their spacing, reconstitution of the fatigue process can be done very thoroughly. Accuracy of the fractographic reconstitution strongly depends on the related a priori information - above all, the relation between macroscopic crack growth rate and striation spacing [5].

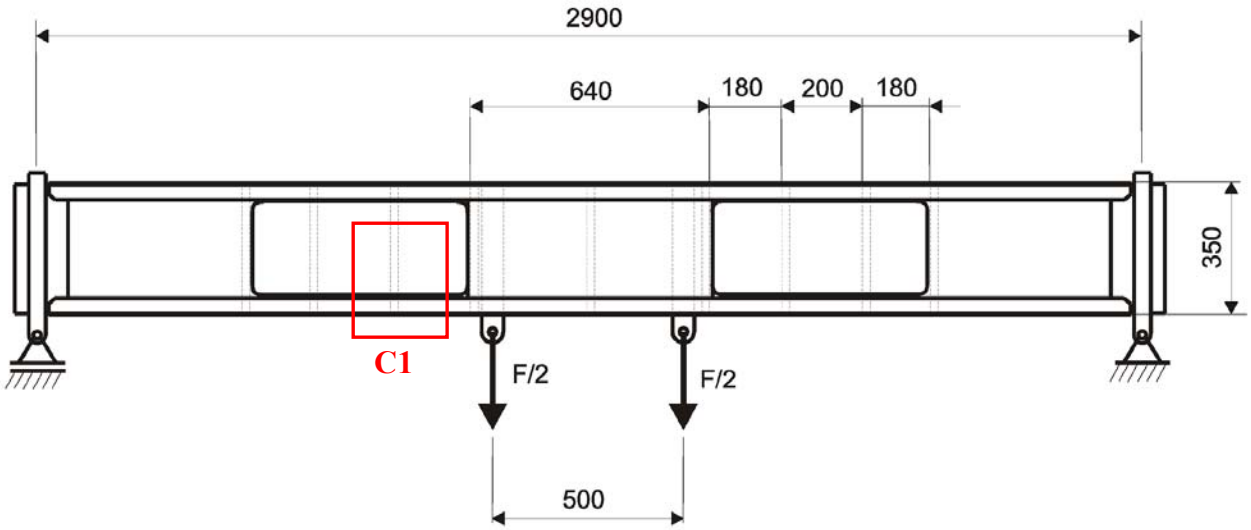

Fig. 1. Four-point bending fatigue test of model wing spar

2 Full-scale fatigue test

Geometry and dimensions of the tested model specimen correspond to the Ayres Loadmaster LM 200 wing spar (Fig.1). The web plate of thickness 1.5 mm was riveted to the L-profile flange plates with dimensions 5x40x40 mm. On both flange plates, sheet strips of 2 mm thickness modeling wing skin were furthermore riveted. All the main structural components of the wing spar were made of Al-alloy type 2124.

The experimental study was focused on the fatigue crack propagation in the spar web [10]. During the period of fatigue tests, the results of which are presented in the paper, four-point bending with constant sinus cycle at stress ratio $R = 0$ and loading frequency $f = 2$ Hz was applied. In the critical area, the loading force induced a stress with $\sigma_{max} = 100$ MPa, which corresponds to the maximal value in loading spectrum applied usually in the fatigue life tests

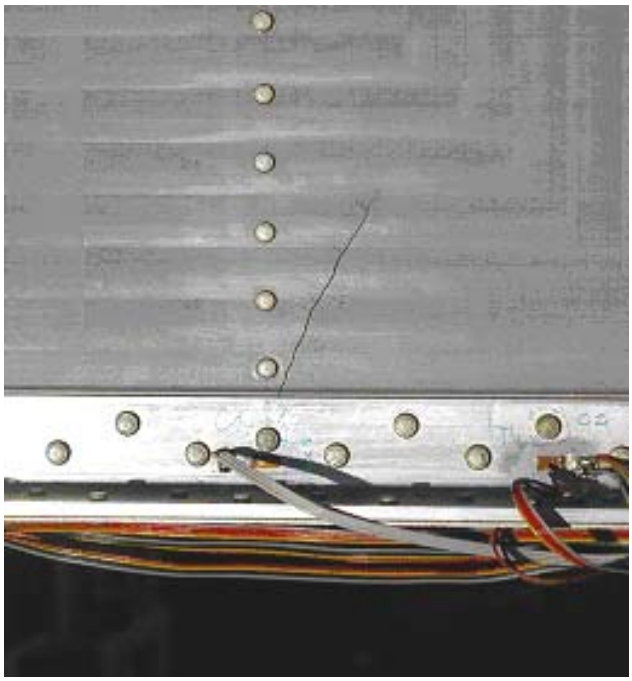

Fig. 2. Critical area C1 - riveted connection of spar web and lower flange plate (after fatigue test finish).

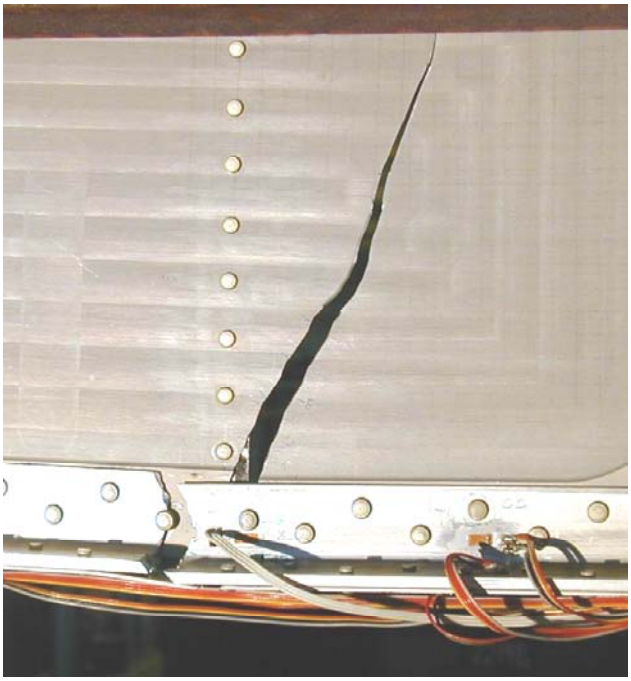

Fig. 3 The same area C1 as in Fig. 2 after following residual strength test.

of similar small transport airplanes. In the critical area (denoted C1– see Fig. 1), artificial notches were cut in rivet holes. The fatigue test of the wing spar was finished after $N = 117\ 500$ applied loading cycles.

3 Direct macroscopic monitoring of fatigue crack growth in area C1 of the wing spar

The fatigue cracks under study initiated on vertical sharp notches in the hole of rivets connected the spar web and the lower flange plate (Figs 2 and 3). During the test, the main fatigue crack propagating upwards in the spar web (denoted C1S2) was optically monitored. In moments of the macroscopic measurements, cyclic loading was interrupted, and the static load was kept on the level corresponding to the maximum of the previous cycle.
The results of two-dimensional measurements on the web surface are summarised in Fig. 4. In the first period of the fatigue test, when the flange plate covered the crack in the spar web, direct monitoring was impossible. This objective reason results in the fact that optical information on growth of the main fatigue crack C1S2 in the web was available only from the last 42% of the test duration. No macroscopic data dealing with the second crack in the web (denoted C1S1) and both cracks in the lower flange plate (C1P1 and C1P2) were obtained.

4 Fractographic analysis of fatigued wing spar components

The limited set of macroscopic data on fatigue crack propagation was completed by fracto-

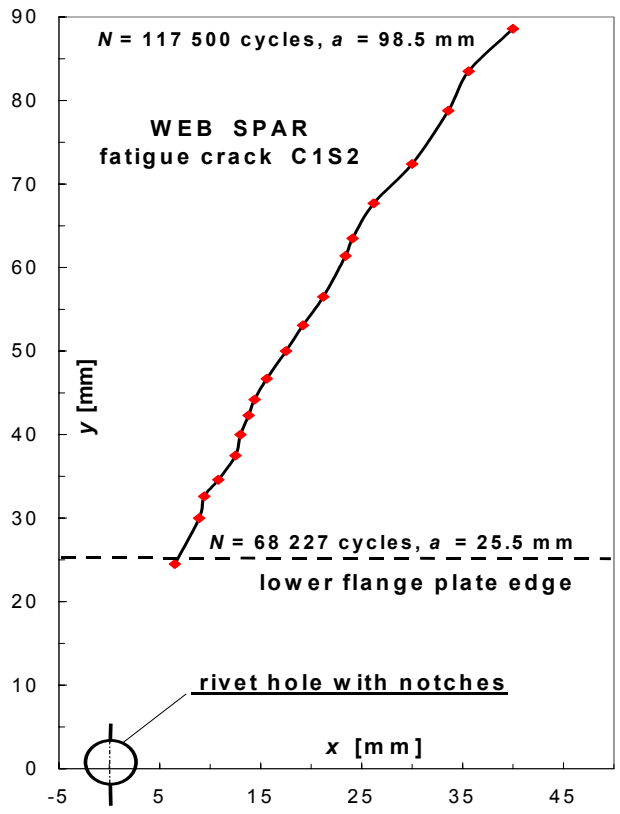

Fig. 4. Results of direct visual monitoring of the fatigue crack C1S2 in the spar web during the test.

graphic results. After dismantling the fractured wing spar, specimens with fatigue cracks both in the web and in the lower flange plate were observed by means of binocular light microscope and scanning electron microscope. Two fatigue cracks in the web and two ones in the lower flange plate were under study. The main results of qualitative and detailed quantitative fractographic analysis of the fracture surfaces are summarised in the following paragraphs.

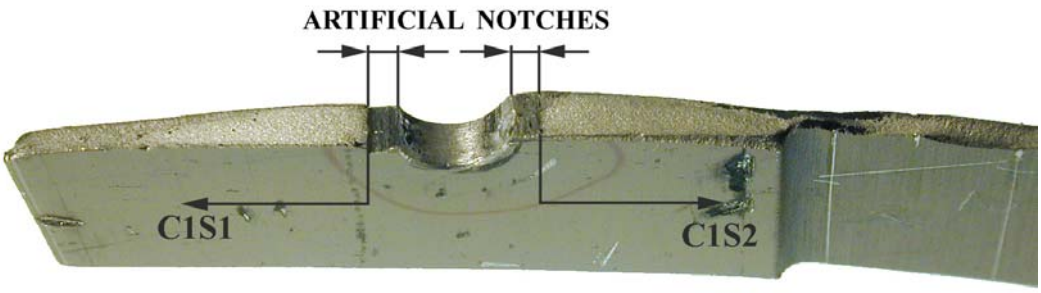

Fig. 5. Two fatigue cracks C1S1 and C1S2 propagated from notched rivet hole in wing spar web.

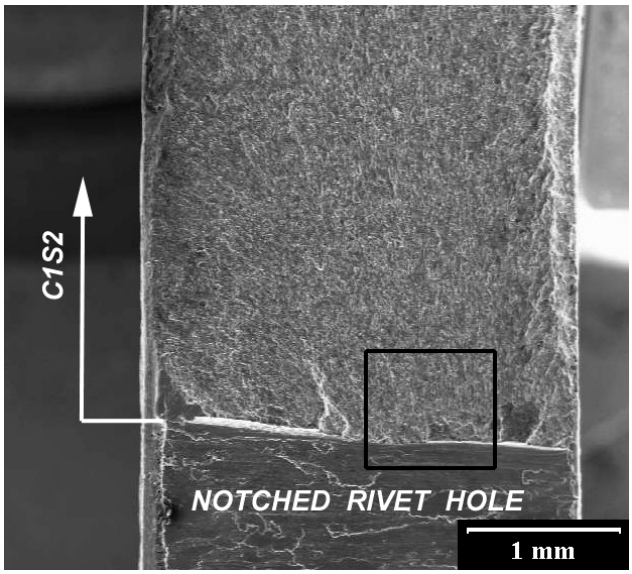

Fig. 6. Initiation of crack C1S2 in web spar.

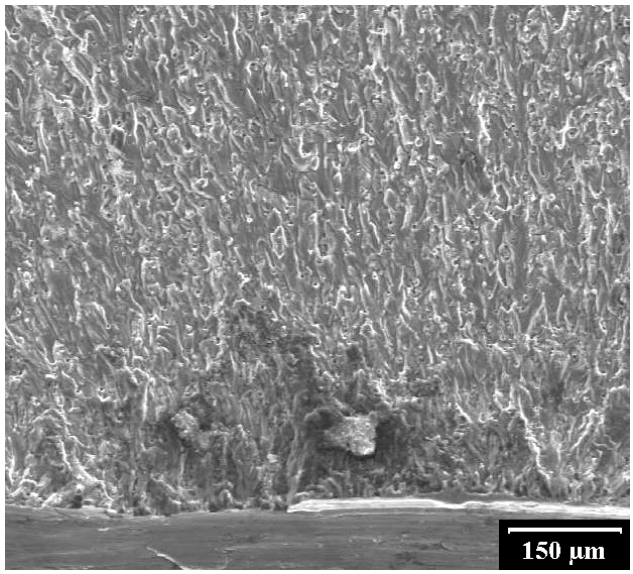

Fig. 7. Detail of initiation site from Fig. 6.

4.1 Qualitative and quantitative fractographic analysis of spar web

In the case of both fatigue cracks in the web (i.e., C1S1 and C1S2 - Fig. 5), initiation on sharp notches in the rivet hole was of a multiple character (see Figs 6 and 7). Striations are a typical microfractographic feature of the cracks, regardless of both crack length and fracture orientation in the web. Striation spacing s was measured and presented as a function of crack length a, where a = distance of micro-area under study and rivet hole axis. Over 700 individual measurements of striation spacing were carried out on the fracture surfaces of the cracks in the spar web.

The quantitative fractographic results are presented and compared in Fig. 8 - each point representing a weighted mean value of about ten striation spacing data at the same crack length. It is evident that both fatigue cracks in the web were propagating at very similar rates. In the same graph, the microfractographic data $s = s(a)$ (open points) are compared with macroscopic crack growth rates $v = v(a)$ (full red points)

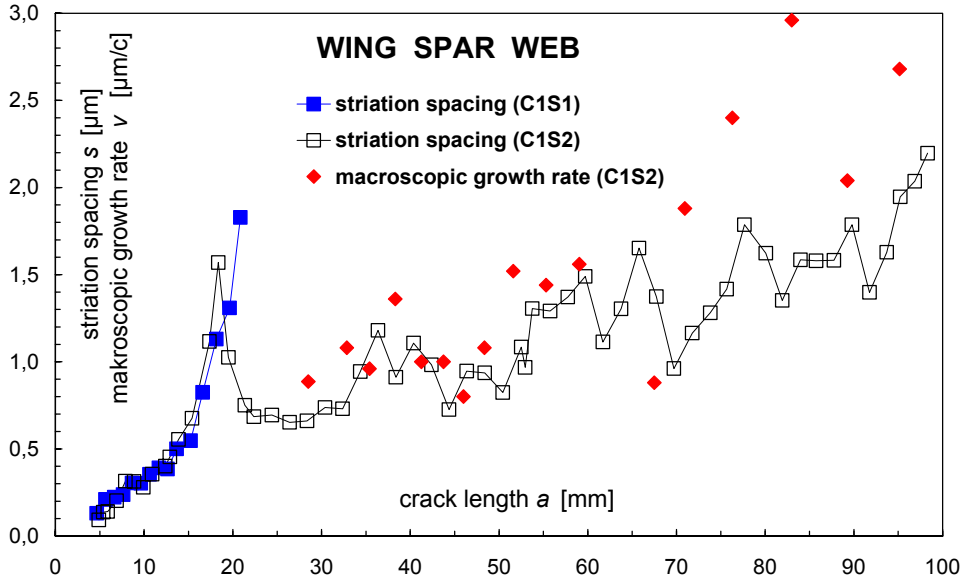

Fig. 8. Spar web : striation spacing and macroscopic crack growth rate vs. crack length.

corresponding to the results of direct optical monitoring (the limited data set only for C1S2 crack - see Fig. 4). For their computation, the secant method was used. The comparison of fractographic and macroscopic data in Fig. 4 is in accordance with general experience [5]:– in the range of middle crack length, equation $v \cong s$ may be approximately acceptable, while for longer cracks, inequality $v > s$ is obvious.

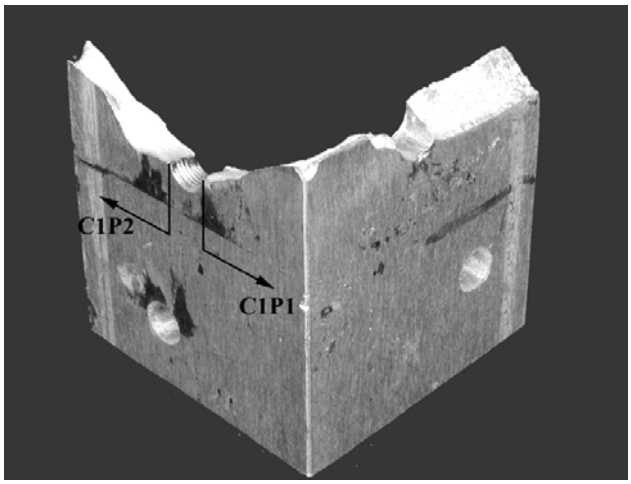

Fig. 9. Fractured lower flange plate with fatigue cracks C1P1 and C1P2.

4.2 Qualitative and quantitative fractographic analysis of lower flange plate

Fatigue cracks C1P1 and C1P2 propagated from the rivet hole located left from the rivet hole

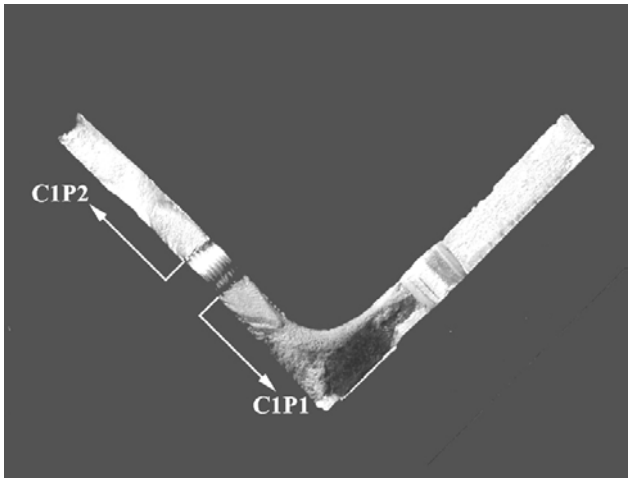

Fig. 10. Fracture surfaces of cracks C1P1 and C1P2 initiated on the rivet hole in lower flange plate.

where the cracks C1S1 andC1S2 in the spar web initiated (see Fig. 3). Both the cracks in the lower flange plate were initiated on the surface roughness (probably drilling traces) in the rivet hole (Fig. 11).
Macroscopically, both the cracks propagated from the corners adjacent to the riveted spar web. Similarly as in the case of cracks in the spar web, the fatigue process was accompanied by striation formation. In Fig. 12, striation spacing s as a function of crack length a is presented for cracks in the flange plate.

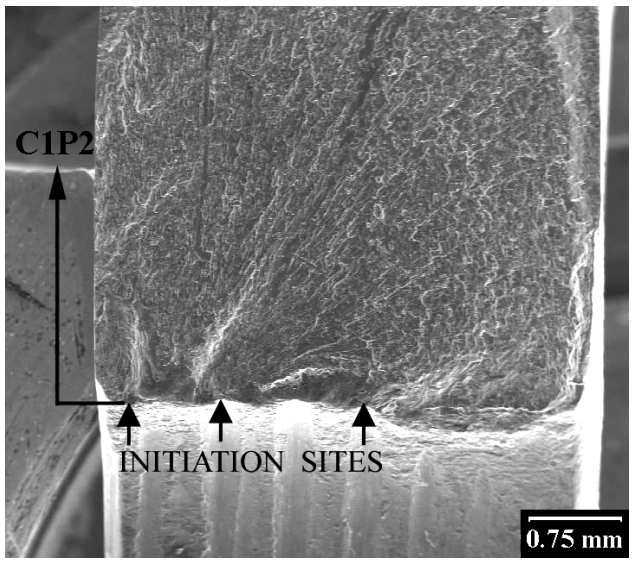

RIVET HOLE IN FLANGE PLATE

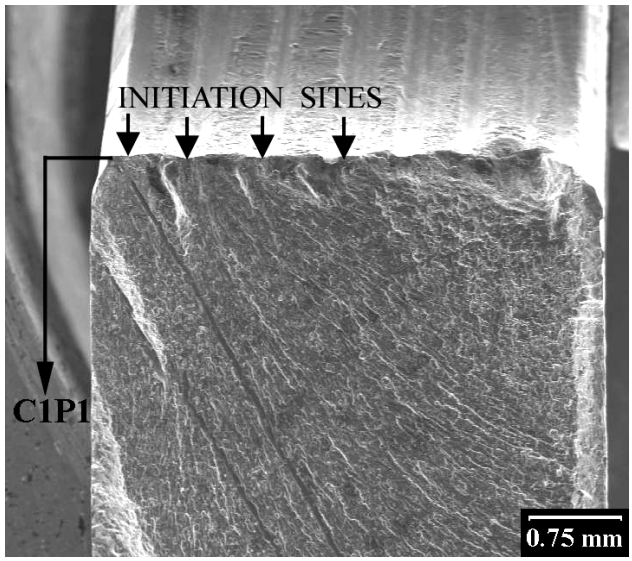

Fig. 11. Multiple initiation of fatigue cracks C1P1 and C1P2 on rivet hole in lower flange plate of the wing spar.

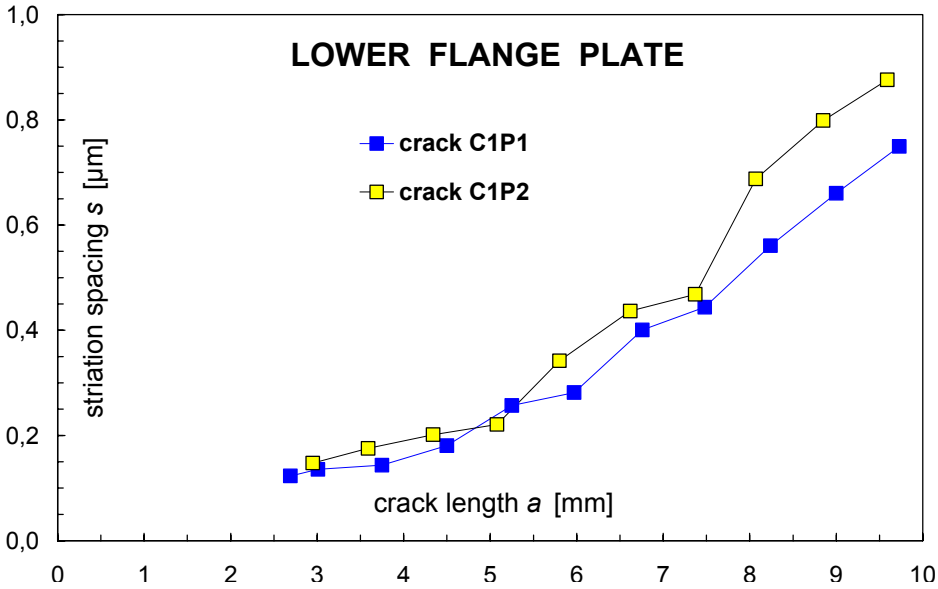

Fig. 12. Cracks C1P1 and C1P2 in lower flange plate : striation spacing vs. crack length.

4.3 Fractographic reconstitution of fatigue crack growth history

Ex-post reconstitution of the fatigue process history was based on the results of quantitative microfractographic analysis, i.e., on the dependence of striation spacing on crack length (s_i, a_i), i = 1,2,...,n. Details of the method used were described previously in [11],[12].

Processing of the data consists of two steps:

a) recalculation of the striation spacing into the macroscopic crack growth rate,

b) integration of the results obtained into the relation of the crack length as a function of the number of applied cycles.

Generally, striation spacing s and macroscopic crack growth rate v cannot be taken as identical. The ratio of the variables

$$D = \frac{v}{s} \qquad (1)$$

can vary within several orders ($10^{-3} < D < 10^{1}$) (see, e.g., [13],[5]). This fact is a consequence of the three following phenomena:

1) Discontinuous propagation of fatigue crack front both in time and in space, i.e., existence of the co called “idle cycles”.

2) Deviation of local direction of fatigue crack growth from the macroscopic one [14],[15].

3) Synergy of striation formation micro-mechanism with other ones, e.g., ductile dimple fracture, inter crystalline decohesion, quasi-cleavage, etc.

An a priori quantitative information on ratio D is very desirable for applications in practice. For these purposes, the most suitable form is relation $D = D(s)$, which can be determined from laboratory tests on simple bodies made of the same material as the fractured structural part under study. Also close correspondence of testing conditions with the service ones is very advisable.

In addition to the above information, knowledge of some couple of corresponding data (a_i, N_i) contributes noticeably to the quality and exactness of final results of fractographic reconstitution. This pair may be given by the number of cycles and corresponding crack length at the moment of service interruption, termination etc.

If $D = D(s)$ and one couple of corresponding data (a_i, N_i) are available, the following equation can be used to reconstitute the fatigue crack growth history

$$N_x = \int_{a_i}^{a_x} \frac{da}{D(s)\cdot s(a)} + N_i, \qquad (2)$$

where N_x is the number of cycles corresponding to the given crack length a_x.

If the *D(s)* relation is not available, knowledge of two couples of corresponding data (a_i, N_i), $i = 1,2$ is required. Provided that $D = v/s = const$ (a priori unknown) in this case, the rough fractographic reconstitution of the fatigue crack growth can be based on the equation [11]

$$N_x = N_1 + (N_2 - N_1) \cdot \frac{\int_{a_i}^{a_x} \frac{da}{s(a)}}{\int_{a_i}^{a_2} \frac{da}{s(a)}}. \qquad (3)$$

As a secondary result, it is possible to determine the value of constant $D = const$

$$D = \frac{1}{N_2 - N_1} \int_{a_i}^{a_2} \frac{da}{s(a)} = const. \qquad (4)$$

Precision and exactness of fractographic reconstitution results strongly depend on the volume and quality of input information. This fact is supported in the following paragraph where the results of fractographic reconstitution based on three various alternative hypotheses are presented and compared.

The same microfractographic input $s = s(a)$ (see Fig. 8) was processed for crack C1S2.

Assumptions of hypothesis H0:

a) knowledge of two pairs of corresponding data (N_i, a_i),
b) $D = v/s$ = unknown constant.

Assumptions of hypothesis H1:

a) knowledge of one pair of corresponding data (N_i, a_i),
b) $D = v/s = 1$ (widely used but usually not verified).

Assumptions of hypothesis H2:

a) knowledge of one pair of corresponding data (N_i, a_i),
b) knowledge of empirical relation $D = D(s)$ based on our previous laboratory experiments of similar Al-alloy [5]:

$$D = 1.797 \cdot 10^{45} \frac{s^{0.1108}}{(79.55 - s)^{23.84}} \qquad (5)$$

for $(0.09 \le s \le 4.74)$ μm.

The known couple of data $N_f = 117\,500$ cycles and $a_f = 98.5$ mm, corresponding to the fatigue test termination, was used as a border condition in these three cases. The second pair of the corresponding data necessary for application of

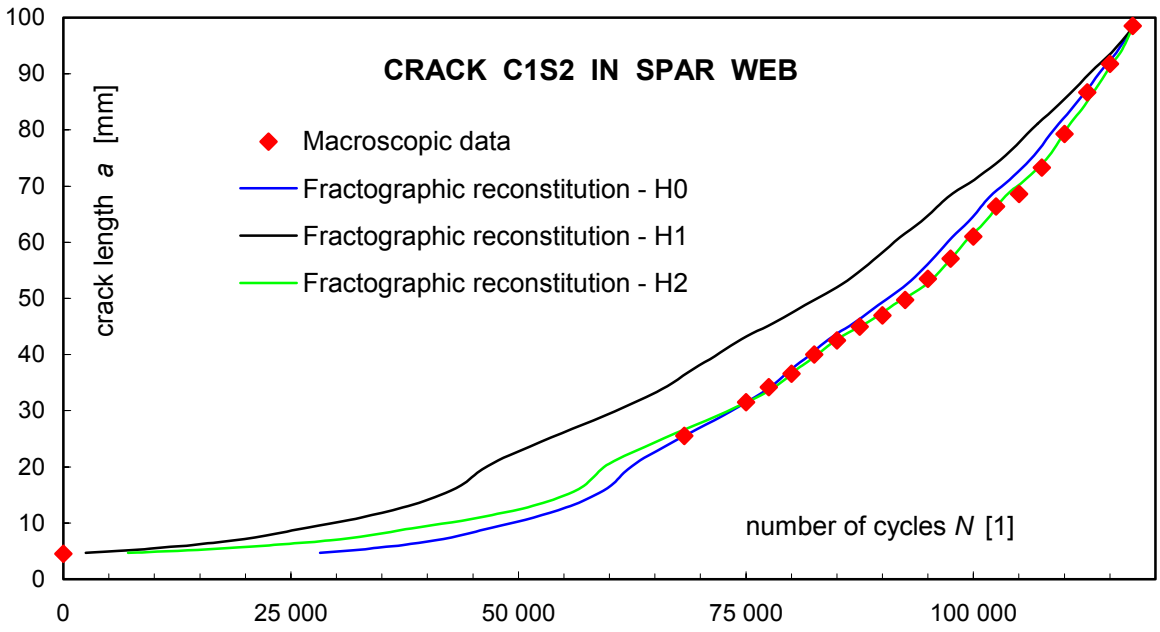

Fig. 13. Comparison of fractographic reconstitution of crack growth curves based on hypotheses H0, H1, and H2 with macroscopic data.

hypothesis H0 was given by crack length $a = 25.5$ mm and $N = 68\ 227$ cycles (see Fig.4). In Fig.13, the three resulting crack growth curves $a = a(N)$, the fractographic reconstitution of which was based on application of the hypotheses H0, H1, or H2, were compared with the discrete macroscopic data (available only in the range $68\ 227 \le N \le 117\ 500$, i.e., $25.5 \le a \le 98.5$ mm – see Fig. 4).

It is evident that application of hypothesis H1 results in the crack growth curve the deviation of which from macroscopic data is unacceptable. It is clear that real macroscopic crack growth rates are higher than the reconstituted ones (see Fig. 13). This disagreement is a consequence of the fact that assumption $D = v/s = 1$ was not fulfilled - in the stage where macroscopic measuring was carried out inequality $v > s$ is valid (see Fig. 6).

Agreement between the results of fractographic reconstitution based on H0 hypothesis and macroscopic data is much better, but in the first stage of the growth it results in the conclusion that crack C1S2 had not propagated before $N_0 \approx 28\ 200$ cycles. Because the crack initiated on the sharp notch, this value seems to be rather higher - it represents about 24% of all the testing time.

However, the best of the three results of fractographic reconstitution is the crack growth curve based on the knowledge of $D(s)$ (hypothesis H2 - Eq. (5)). In this case, the agreement with macroscopic data is excellent and estimation of number of cycles corresponding to crack initiation is realistic value $N_0 \approx 6\ 900$ cycles.

Fractographic reconstitution of growth history of the second crack C1S1 in the spar web and both cracks C1P1 and C1P2 in the lower flange plate was based also on application of hypothesis H2, incorporating the relation between the macroscopic crack growth rate and striation spacing in the form of empirical relation (5). No couples of macroscopic corresponding data (a_i, N_i) were available for these three cracks. The missing information was substituted by the assumption that cracks C1S1 and C1S2 initiated in the spar web at the same moment, and cracks C1P1 and C1P2 in the flange plate propagated until the fatigue test termination.

The results of fractographic reconstitution for all four fatigue cracks in the wing spar critical area under study are summarized in Fig. 14. In the same plot, the limited macroscopic data set is presented. This synoptic presentation offers complex information on the time sequence of individual cracks and their interaction.

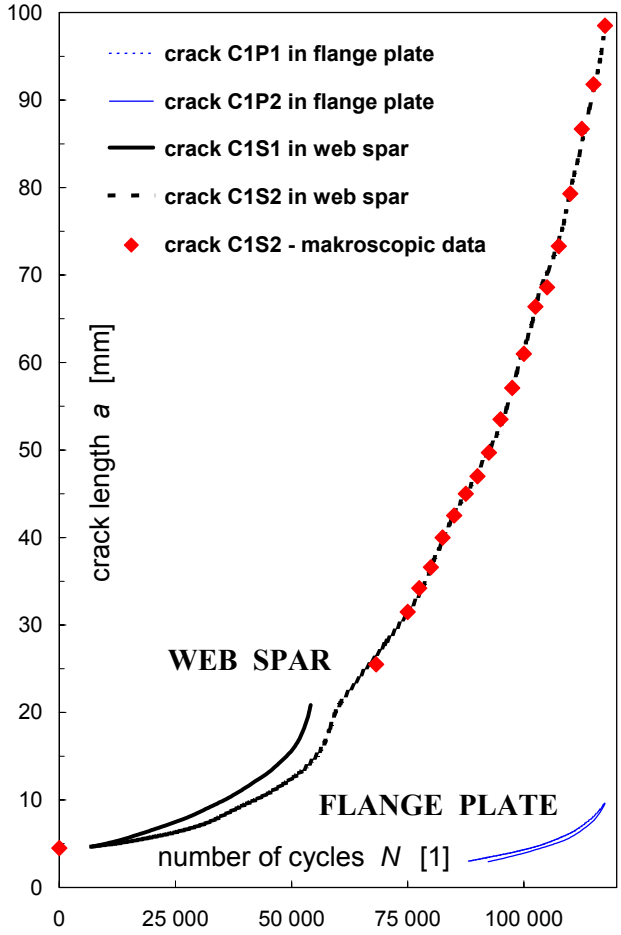

Fig. 14. Summary of results of fractographic reconstitution and visual macroscopic monitoring of four fatigue cracks in wing spar critical area.

The technique of visual macroscopic monitoring can negatively affect the results of fatigue tests: The measurements of crack length were carried out at static load equal to the maximum of fatigue cycle. Both the fractographic reconstitution and the direct macroscopic crack growth rate vs. the crack length of C1S2 are presented in Fig. 15.

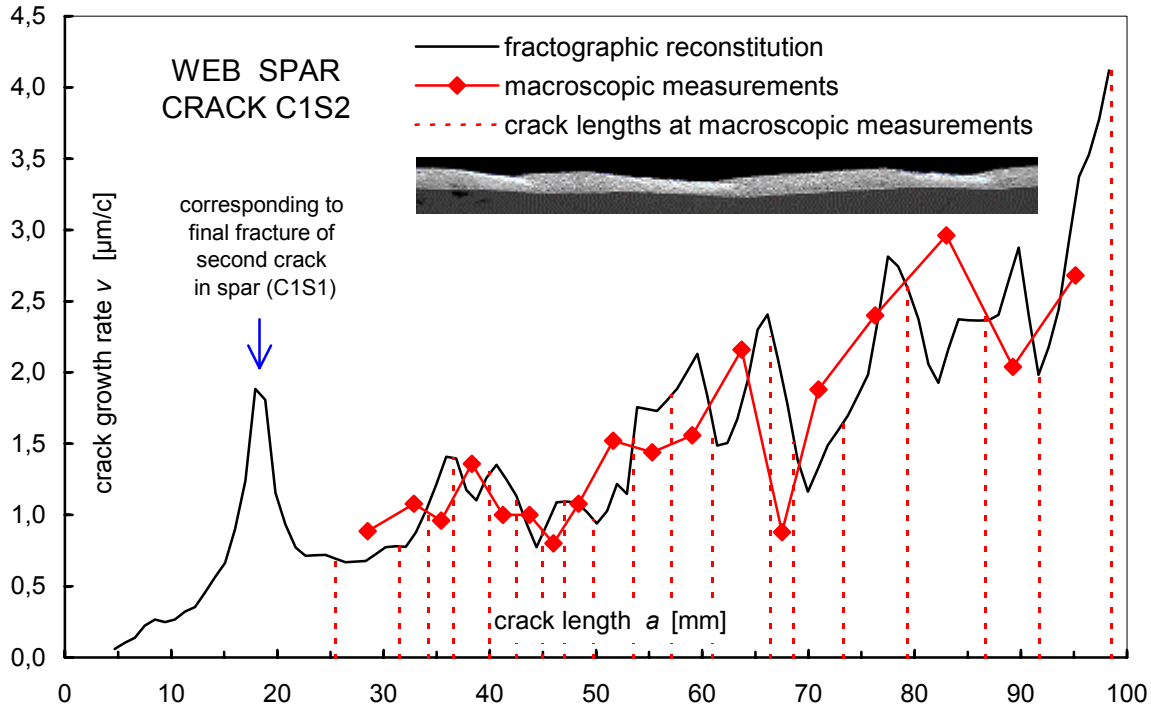

Fig. 15. Comparison of fractographic reconstitution of relation crack growth rate vs. crack length with macroscopic data. Influence of monitoring method applied is visible.

Similarly as in Figs 13 and 14, good agreement between both data sets is demonstrable. The crack lengths, at which direct macroscopic measurements were carried out, are given by dashed lines in this graph. In the vicinity of these points, a slope of the relation $v(a)$ usually noticeably changes. This correlation outlines an influence of static loading during the visual measurements on fatigue crack growth. This opinion is in agreement with macro-fractographic findings: orientation of the main macroscopic plane of the fracture often varies due to static load during the macroscopic measurements (see photo embedded in Fig. 15).

5. Conclusions

Fatigue crack growth rate is one of the most important critical parameters in the lifespan and risk calculation [16]. Due to initiation and growth in hidden parts or in an area inaccessible to routine visual monitoring, macroscopic data can be very limited and inaccurate. The missing required information can be obtained by means of post-test fractographic reconstitution of fatigue crack growth history. Quantitative fractography has played a substantial role in the destructive evaluation and full-scale fatigue testing of both the new proposed and the aging aircraft components [17],[18]. This technique is a very useful tool also in service failure analysis. In similar cases, fractographic methods can offer detailed and exact knowledge of the structure response to the time variable loading. Information of this type is often unattainable by any other means.

Precision of the fractographic reconstitution strongly depends on the amount and credibility of input data. An uncritical application of $v = s$ can lead to distorted information on fatigue process history. An a priori knowledge of the relation between macroscopic crack growth rate v and striation spacing s is of a crucial importance. The practical significance of D-factor was demonstrated elsewhere, e.g., in [19]. Relation $v = D.s$ must be verified experimentally under conditions similar to service ones. Another important factor is the knowledge of at least one couple of corresponding data (a_i, N_i), which enables to locate the reconstitution results in exploitation time. This aspect can be successfully solved by fracture marking.

Fractographic reconstitution method based on striation spacing was applied in the fatigue evaluation of the model wing spar. By this technique, information on initiation, propagation, time-sequence, and interaction of four fatigue cracks in the spar critical area has been obtained. In the case of the crack, the growth of which was visually monitored during the test, the results of fractographic reconstitution are in very good agreement with the macroscopic ones. For the three other fatigue cracks under study, hidden and inaccessible to direct observation, fractographic data represent the only information on their growth history.

Analysis of the data obtained has suggested that the applied method of direct visual monitoring can affect the fatigue process. This artifact would negatively influence the reliability and reproducibility of full-scale test results.

Acknoledgement

This work has been supported by the grant of Czech Science Foundation No. 101/98/029, and by the project CEZ:J04-98:210000021.

References

[1] Anon.: *Federal Aviation Regulation*. Part 25 Airworthiness Standards: Transport Category Airplanes. Sec. 25.571 Damage-Tolerance and Fatigue Evaluation of Structure. FAA, 1978.

[2] Kunz J, Nedbal I and Siegl J. Application of fractography in full-scale tests of aircraft structure parts. *Proc ECF 8,* Torino (Italy), Vol. I, pp 1662-1669, 1990.

[3] Kunz J, Nedbal I, Siegl J and Pártl O. Fractographic remarks to fatigue crack growth rate. *Proc. Fatigue 93*, Montreal (Canada), Vol. II, pp 649-654.

[4] Schijve J. The significance of fractography for investigations of fatigue crack growth under variable-amplitude loading. *Fatigue Fracture Engineering Materials Structures*, Vol. 22, No. 2, pp 87-99.

[5] Nedbal I, Siegl J and Kunz J. Relation between striation spacing and fatigue crack growth rate in Al-alloy sheets. *Proc ICF 7,* Houston (USA), Vol. 5, pp 3483-3491, 1989.

[6] Siegl J, Schijve J and Padmadinata U H. Fractographic observations and predictions on fatigue crack growth in an aluminium alloy under miniTWIST flight-simulation loading. *Int. J. Fatigue*, Vol. 13, No. 2, pp 139-147, 1991.

[7] Nedbal I, Kunz J and Siegl J. Some remarks on fatigue fracture marking. *Proc. Fatigue '99*, Beijing (China), Vol. 4/4, pp 2373-2378, 1999.

[8] Dainty R V. Use of "marker blocks" as an aid in quantitative fractography in full-scale aircraft fatigue testing: A case study. *Fractography of ceramics and metal failures, ASTM STP 827*, pp 285-308, 1984.

[9] Willard S A. Use of marker bands for determination of fatigue crack growth rates and crack front shapes in pre-corroded coupons. *NASA/CR-97-206291*, 1997.

[10] Augustin P and Píštěk A. Experimental data determination for the damage tolerance analysis of the wing spar with cracked web. *Proc 38th Int. conf. EAN 2000,* Třešť (Czech Republic), pp 9-14, 2000.

[11] Nedbal I, Siegl J and Kunz J. Fractographic Study of Fatigue Crack Kinetics in Bodies and Structures. *Proc. ICF 6,* New Delhi (India), Vol. III, pp 2033-2040, 1984.

[12] Nedbal I, Kunz J and Siegl J. Quantitative Fractography - Possibilities and Applications in Aircraft Research. *Proc. Basic Mechanisms in Fatigue of Materials*, Brno (Czech Republic), pp 393-403, 1988.

[13] Roven H J, Langøy M A, and Nes E. Striations and the Fatigue Growth Mechanism in a Micro-Alloyed Steel. *Proc. Fatigue '87*, Charlottesville (USA), Vol. I, pp 175-184, 1987.

[14] Nedbal I, Kunz J and Siegl J. Microfractographic aspects of fatigue crack growth in 7010 aluminium alloy. *Proc. Fractography '97*, Stará Lesná (Slovakia), pp 264-270, 1997.

[15] Kunz J, Nedbal I and Siegl J. Local Directions of Fatigue Crack Propagation in Microvolume of Aluminium Alloy 7010. *CTU Reports, Proc. Workshop 2003*, *Part B*, Prague (Czech Republic), Vol. 7, pp 594-595, 2003.

[16] White P, Barter S and Molent L. Probabilistic fracture prediction based on aircraft specific fatigue test data. *6th Joint FAA/DoD/NASA Aging Aircraft Conference*, San Francisco (California, USA), pp 1-21, 2002.

[17] Seher Ch, Smith Ch. Managing the aging aircraft problem. *AVT Symposium on Aging Mechanisms and Control and the Specialists Meeting on Life Management Techniques for Aging Air Vehicles*, Manchester (England), pp 1-7, 2001.

[18] Bakuckas J G Jr and Carter A. Destructive evaluation and extended fatigue testing of retired aircraft fuselage structure: project update. Proc. 7th *Joint FAA/DoD/NASA Conference on Aging Aircraft*, New Orleans (Louisiana, USA), pp 1-12, 2003.

[19] de Matos P F P, Moreira P M G P, Nedbal I and de Castro P M S T. Fractographic study of fatigue crack surfaces in open-hole specimens. *Proc. 9th Portuguese conf. on fracture*, Setúbal (Portugal), pp 91-99, 2004 (CD-ROM).